



# The topology of electronic band structures

Prineha Narang<sup>1</sup><sup>✉</sup>, Christina A. C. Garcia<sup>1</sup> and Claudia Felser<sup>1,2</sup>

**The study of topology as it relates to physical systems has rapidly accelerated during the past decade. Critical to the realization of new topological phases is an understanding of the materials that exhibit them and precise control of the materials chemistry. The convergence of new theoretical methods using symmetry indicators to identify topological material candidates and the synthesis of high-quality single crystals plays a key role, warranting discussion and context at an accessible level. This Perspective provides a broad introduction to topological phases, their known properties, and material realizations. We focus on recent work in topological Weyl and Dirac semimetals, with a particular emphasis on magnetic Weyl semimetals and emergent fermions in chiral crystals and their extreme responses to excitations, and we highlight areas where the field can continue to make remarkable discoveries. We further examine open questions and directions for the topological materials science community to pursue, including exploration of non-equilibrium properties of Weyl semimetals and cavity-dressed topological materials.**

Materials are essential and ubiquitous, playing a critical role in our daily lives. Materials are also a key component of basic science, as demonstrated by the numerous Nobel Prizes awarded for the discovery and design of materials. Each prize has heralded an era in materials science, with prominent examples including the Nobel Prize in Physics in 1987 awarded for the discovery of high-temperature superconductivity in copper-oxide-based materials<sup>1</sup> that spurred decades of research in high-critical-temperature materials, in 2007 for the discovery of giant magnetoresistance<sup>2</sup> that revolutionized information storage and led to immense research in magnetic materials, in 2010 for experiments on graphene<sup>3</sup> that opened up the active field of two-dimensional (2D) materials science, and in 2014 for the invention of bright blue light-emitting diodes<sup>4</sup> that enable energy-saving white light sources. The prize in 2016 for the theoretical introduction of topological phase transitions and phases of matter<sup>5</sup> recognized the work that ushered in an era of topological materials science.

Many discoveries in condensed matter physics rely largely on new connections between topology and electronic structure. Topology is the branch of mathematics, which is concerned with continuous deformations of geometric objects, for example, stretching or twisting but not tearing or breaking. A topological or topologically non-trivial material is one whose electronic or magnetic structure has features akin to knots or twists that cannot be untangled without breaking or changing the fundamental nature of the material. Topological materials science as a field is about finding, making and exploring properties of materials that can be understood more deeply under this lens, that is, in connecting the topologies of electronic and magnetic structures in reciprocal and real space to physical observables. New classes of quantum materials have been found in insulators and semimetals that exhibit non-trivial topologies, and these materials display a plethora of phenomena, including topological surface states; fermionic excitations such as Weyl, Dirac or Majorana; and non-collinear spin textures such as skyrmions. A hallmark of many of these quantum properties, which are derived from fundamental symmetries of the bulk, is that they are topologically protected, and some can be directly tied to non-equilibrium phenomena and extreme responses to external stimuli.

In the field of topologically non-trivial matter, theory very often guides experiments, both in predicting new phenomena and in discovering new materials. Most notably, advances in electronic band theory using symmetry indicators and the link between topology and local chemical bonding have allowed for the broad prediction and classification of the topology of electronic states of 2D and three-dimensional (3D) materials<sup>6–9</sup>. Computational searches employing topological quantum chemistry and other symmetry-driven methods, along with high-throughput density functional theory calculations and catalogued crystallographic symmetry information, have examined the band topology of over 26,000 materials<sup>10–12</sup>, finding that roughly 27% of materials are likely to be topologically non-trivial. These searches tell us that there are likely to be many more materials with topologically non-trivial electronic structure than previously imagined, given the relatively small pool of materials experimentally determined to exhibit this property to date. Equally interesting is the observation that while some of the compounds uncovered by these methods are yet to be realized or very recently synthesized, some of them have been studied for decades, and interpretation of their properties in topological terms has offered new insights. Topological quantum chemistry and other methods fill an essential gap in the discovery of materials by directly linking chemical compositions to topological properties. The next steps in the discovery of topologically non-trivial materials must involve developing design principles beyond the heuristics and compositional intuition of materials chemistry in order to assist in the discovery of materials with specific, optimized properties fully exploiting their topological nature.

## Topological insulators

The classification of materials according to the topology of their respective electronic structures began with the discovery of topological insulating states arising from the spin–orbit interaction<sup>13–17</sup>. Band structure topology was found to become non-trivial in materials with large spin–orbit coupling if the conduction and valence bands are inverted, as explained and shown in Box 1. The inversion of the 6s states of Hg and 5p states of Te in HgTe is a prominent example of such a band inversion and can be alternatively viewed as a consequence of the inert pair effect in chemistry, which is the propensity for the two electrons in the outermost s orbital to

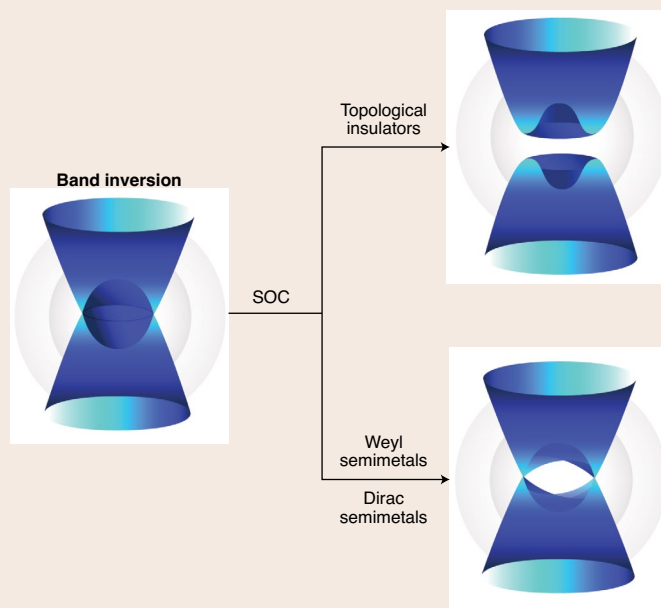
<sup>1</sup>John A. Paulson School of Engineering and Applied Sciences, Harvard University, Cambridge, MA, USA. <sup>2</sup>Max-Planck-Institut für Chemische Physik fester Stoffe, Dresden, Germany. ✉e-mail: [prineha@seas.harvard.edu](mailto:prineha@seas.harvard.edu)

**Box 1 | Explaining band inversion and the emergence of topology in materials**

An insulator is a material with a large energy gap between its conduction and valence bands, usually prohibiting conventional electrical conduction. Depending on the size of the gap, these materials will be transparent, white or of a certain visible colour, which indicates the wavelength of light absorption in the material. Semiconductors, which can be made to conduct under certain conditions, are materials with small bandgaps, and semimetals are materials with slightly overlapping bandgaps in different parts of the Brillouin zone. Because semimetals are not fully gapped, incoming light will be easily absorbed and quickly reemitted as in metals; as a consequence, these materials are typically black in colour and shiny.

In many ionic and semiconducting materials, the *s* electrons form the conduction band while the *p* or *d* electrons build the valence band. However, if the materials contain heavy elements, due to relativistic effects, the outer *s* electrons of the heavy elements can be lower in energy compared to the *p* or *d* electrons of the light elements. The result is a semimetal with overlapping conduction and valence bands that have been ‘inverted’ in terms of their energies and orbital characters (Box 1 figure, left), with a band crossing that is referred to as a nodal line. If this nodal line becomes gapped due to spin–orbit coupling, either fully as in topological insulators (Box 1 figure, top right) or everywhere except at certain points in the Brillouin zone as in Weyl and Dirac semimetals (Box 1 figure, bottom right), this band inversion still remains and results in non-trivial topology of the electronic structure. This is due to the band inversion playing a role in the Berry connection, the gauge potential associated with the Berry phase of the Bloch wave functions. In topological insulators, the Berry phase is quantized and directly corresponds to non-trivial topological description. In Weyl semimetals, the Berry curvature, the corresponding gauge field, diverges at the Weyl points, which are thus described also as monopoles and antimonopoles of Berry curvature in momentum space, with the integral of the Berry curvature over a sphere surrounding one Weyl node being equal to  $\pm 1$ . The Weyl semimetal phase, assuming momentum is still conserved, can only be gapped out if these monopoles and antimonopoles come together; in this way, the Weyl semimetal is

topologically non-trivial. Thus, this mechanism of band inversion is the reason that many topologically non-trivial materials known today contain heavy elements.



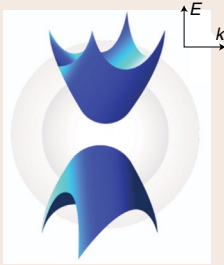
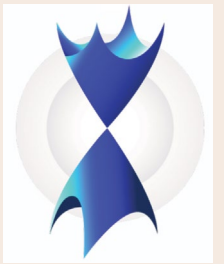

**Band inversion.** Band inversion (left) facilitates the formation of topological insulators (top right) and Weyl and Dirac semimetals (bottom right). Overlapping valence and conduction bands of different orbital characters form a nodal line in the Brillouin zone where the bands cross in energy. Spin–orbit coupling can open a full energy gap, resulting in a topological insulator, or everywhere along the nodal line except for at special points, called Weyl or Dirac points, in Weyl and Dirac semimetals. In all of these cases, the band inversion stemming from the overlapping bands without spin–orbit coupling results in the non-trivial topology of these electronic structures. Figure adapted with permission from ref. <sup>90</sup>, Annual Reviews.

remain unionized in heavier elements. In a class of insulators with topologically non-trivial band structure, known as topological insulators (TIs), the surface is metallic despite the bulk being insulating. The surface states of a TI contain 2D Dirac points, named as such because the Hamiltonian describing low-energy excitations near these points in momentum space can be written as the Dirac Hamiltonian for massless Dirac fermions in two dimensions. At these points, the energy disperses linearly with momentum, and the spin and momentum are locked to each other. These states are topologically protected, that is, stable against disorder so long as the overall topology of the electronic structure does not change, when the surrounding space (vacuum or normal insulator) is topologically trivial. TIs can be identified in the bulk band structure by determining the  $Z_2$  topological invariant, which can take only two values, 0 or 1 for topologically trivial and non-trivial states, respectively (see classification in Table 1). This calculation is done, for example, by employing the parity criteria<sup>18</sup>.

Since the predictions of protected edge and surface states in graphene<sup>19</sup> and HgTe quantum wells<sup>20</sup>, topologically non-trivial surface states indicative of TIs have been observed in many materials, including HgTe quantum wells<sup>21</sup> and  $\text{Bi}_2\text{Se}_3$  (refs. <sup>22,23</sup>). Many half-Heusler compounds were also identified as TIs by their band

inversion analogous to that of HgTe, but with additional functionalities such as superconductivity, magnetism and the Kondo effect<sup>24,25</sup>. Ultrahigh mobilities, large magnetoresistance effects, and low bandgaps were all discovered in addition to superconductivity in high-quality single crystals of several materials in the half-Heusler family of YPtBi and LuPtBi (ref. <sup>26</sup>), showcasing the versatility of these compounds beyond their topologically non-trivial nature. Weak TIs can be recognized as quantum spin Hall insulators stacked in three dimensions, with 2D Dirac cones existing only for certain surfaces. Therefore, these materials can be identified by the sensitivity of the metallic surface states to the cleaving surface. These have been identified in layered bismuth compounds such as  $\text{Bi}_{14}\text{Rh}_3\text{I}_9$  (ref. <sup>27</sup>) and  $\text{Bi}_2\text{TeI}$  and in layered variants of the half-Heusler compounds such as  $\text{KHgSb}$  (ref. <sup>28</sup>), which has subsequently become a prominent host of hourglass fermions<sup>29</sup>, surface states that are protected by non-symmorphic symmetries and gain their name from the shape of their dispersions. Beyond bismuth-based and half-Heusler compounds that lack strong electronic correlations, predicted correlated TIs include the actinide materials<sup>30</sup>, correlated skutterudites<sup>31</sup> and  $\text{BaBiO}_3$  (ref. <sup>32</sup>). In addition, there has been much work in recent years exploring the quantum anomalous Hall effect (QAHE) and axion insulator phase in magnetic TIs, including magnetically

**Table 1 | Classification of topological materials**

|  | Classification                | Symmetry                               | Band inversion              |
|--|-------------------------------|--|-----------------------------|
| Topological insulators<br>    | $Z_2$                         | Time reversal                          | Odd times                   |
|  | High order                    | Crystalline symmetry                   | Even times                  |
|  | Crystalline TI                | Crystalline symmetry                   | $\geq 1$                    |
| Dirac and Weyl semimetals<br> | Classification                | Symmetry                               | Band crossing               |
|  | Dirac semimetal               | Rotation                               | Rotation axis               |
|  | Weyl semimetal (non-magnetic) | Inversion symmetry broken              | Accidental degenerate point |
| Weyl semimetal (ferromagnetic)   | Time reversal broken          |  |                             |
| New fermions<br>             | Nodal line semimetal          | Mirror                                 | Mirror plans                |
|  |                               | Non-symmorphic                         | Brillouin zone edge         |
|  | New fermion                   | Rotation and non-symmorphic            | High-symmetry point         |
| Chiral topology  | Mirror symmetry broken        | Arbitrary point (chiral Weyl fermion)  |                             |
|  |                               | High-symmetry point (multiple Fermion) |                             |

A summary of the classification of topologically non-trivial materials by electronic structure and material symmetry. The left-most column of schematics represents the electronic dispersion characteristic of (top to bottom) topological insulators (TIs), Dirac and Weyl semimetals, and materials hosting new fermions that lack high-energy counterparts.

doped and intrinsically ferromagnetic and antiferromagnetic TIs. For an overview of these explorations, see the review in ref. <sup>33</sup>.

### Weyl and Dirac semimetals

Following the excitement surrounding TIs and its implication of new topologically protected electronic states came the predictions of 3D Weyl<sup>34,35</sup> and Dirac<sup>36,37</sup> semimetals. In these materials, the bulk states near the Fermi energy contain twofold and fourfold degenerate band crossings at Weyl and Dirac nodes, respectively. In the vicinity of these nodes, the dispersion is linear in momentum in all three spatial directions; thus, low-energy excitations near these nodes can be described quasi-relativistically by the Weyl and Dirac Hamiltonians. In Weyl semimetals, these nodes come in pairs of opposite chirality, or handedness, corresponding to the two forms of the Weyl Hamiltonian and can be alternatively defined as Berry curvature monopoles and antimonopoles, or sources and sinks, in momentum space (Box 1). The projections of these nodes on the surface are connected by topologically protected Fermi arc surface states. In Dirac semimetals, the 3D Dirac nodes are achiral, as they are the sum of two Weyl nodes of opposite chirality at the same energy and momentum. This makeup of Dirac nodes allows for Fermi arc surface states in Dirac semimetals as well. Prominent examples of well-studied Weyl semimetals include the TaAs family<sup>38–41</sup> and  $T_d$ -MoTe<sub>2</sub> (ref. <sup>42</sup>), both non-magnetic and non-centrosymmetric, and of Dirac semimetals, Na<sub>3</sub>Bi (refs. <sup>37,43</sup>) and Cd<sub>3</sub>As<sub>2</sub> (ref. <sup>44</sup>). Figure 1 highlights how the Dirac and Weyl

physics that underlies these semimetals has a growing role in topological materials science.

The differences between Weyl and Dirac semimetals, related to the chirality or achirality of their respective nodes, come from symmetry (Table 1). Under both time-reversal symmetry and spatial inversion symmetry, every state in the Brillouin zone is at least doubly degenerate due to Kramers' theorem. Both of these symmetries are upheld in a Dirac semimetal, thus Dirac points exist only along high symmetry directions. However, breaking at least one of these symmetries in a material can generate a Weyl semimetal. Thus, one can think of transforming a Dirac semimetal into a Weyl semimetal by breaking one of these symmetries, splitting one achiral Dirac node into two chiral Weyl nodes. In addition, unlike Weyl semimetals, Dirac semimetals are not protected topologically but only by underlying crystallographic symmetry and otherwise become gapped. This is because in a Dirac semimetal, the Weyl nodes, whose chiralities are directly related to positive or negative topological charges, are already brought together at Dirac nodes and sum to zero. Thus, the topological charge is zero everywhere in momentum space, and the Dirac semimetal is topologically trivial. These differences in symmetry and topology have direct and profound consequences on the properties of these semimetals.

Due to their topological protection, Weyl semimetals can be identified using methods that do not apply to Dirac semimetals. An important parameter used to identify these materials theoretically is the Chern number, which in topological materials science is the

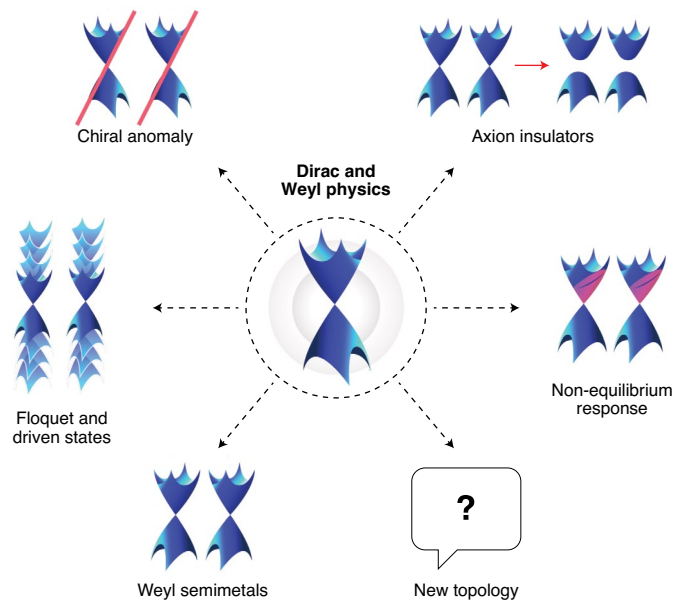


**Fig. 1 | Dirac and Weyl physics.** Dirac and Weyl physics is ubiquitous in topological materials science and related phenomena. Because the dispersion near Dirac and Weyl points is linear in momentum (centre; shown in two dimensions in momentum space for conceptual clarity), the low-energy excitations near these band touchings are well described by the Dirac and Weyl Hamiltonians, respectively. In Weyl semimetals (bottom left), Weyl nodes come in pairs of opposite chirality in momentum space, and the separation of oppositely handed nodes is what protects the Weyl semimetal phase topologically. The existence of chiral fermions (top left) in a Weyl semimetal suggests that these materials and certain driven Dirac semimetals will exhibit the chiral anomaly, which can manifest in a so-called chiral magnetic effect when the material is in the presence of parallel electric and magnetic fields. In addition, Weyl nodes can be induced or moved in energy and/or momentum by electromagnetic driving, allowing for Floquet (periodically driven) Weyl phases (middle left) and non-equilibrium responses (middle right; out-of-equilibrium electrons illustrated in red). In the presence of correlations, a Weyl semimetal can be gapped into a less-explored topological phase, the axion insulator (top right). We similarly expect Dirac and Weyl physics to filter into new topological phases (bottom right) that are continuing to be discovered.

integral of the Berry curvature over a surface (Box 1). The sphere surrounding a Weyl node in momentum space will have a Chern number of  $\pm 1$ , and the Fermi arc is a manifestation of the chiral edge states of the Chern insulator planes that enclose the node. A perhaps more tangible signature of a Weyl semimetal, which has been explored extensively by experimentalists for the TaAs family, is the chiral magnetic effect, a result of the chiral anomaly (Fig. 1). The chiral anomaly is a phenomenon well known in relativistic quantum field theory in which the number of particles of each chirality are not separately conserved due to the presence of a topologically non-trivial gauge field<sup>45–47</sup>. In Weyl semimetals and certain driven Dirac semimetals, the chiral anomaly is predicted to lead to a negative magnetoresistance through the chiral magnetic effect due to the chiral zero modes of the Landau levels at the Weyl nodes and thus can be detected in transport measurements. A critical component in these measurements is the ability to synthesize high-quality samples. We would like to highlight here that there is tremendous opportunity for new materials chemistry approaches to enter the field of topological materials science to diversify the synthesis methods and chemistries accessible.

### Magnetic Weyl semimetals

Though the first experimentally observed Weyl semimetal, TaAs, is a non-magnetic and non-centrosymmetric material (breaking

spatial inversion symmetry), the first predicted Weyl semimetals were magnetic, namely, the pyrochlore iridate  $\text{Y}_2\text{Ir}_2\text{O}_7$  (ref. <sup>34</sup>) and  $\text{HgCr}_2\text{Se}_4$  (ref. <sup>48</sup>). While  $\text{HgCr}_2\text{Se}_4$  has yet to show a Weyl semimetal phase experimentally, some of the pyrochlore iridates have since shown signatures of the phase in transport experiments<sup>49–51</sup>, and there has been much more work in just the past few years that has identified other magnetic Weyl semimetals. These include the LnPtBi family of half-Heusler compounds, wherein Weyl nodes can be induced via a magnetic exchange field. GdPtBi and NdPtBi have been shown to become Weyl semimetals only in applied fields of the order of  $\sim 2$  T (refs. <sup>52,53</sup>), and both compounds show two strong signatures of the chiral anomaly that are absent in their non-magnetic analogue YPtBi: a large unsaturated negative quadratic magnetoresistance for fields up to 60 T and an unusual intrinsic anomalous Hall effect (AHE)<sup>53</sup>.

In the large family of magnetic full-Heusler compounds, Weyl nodes are predicted to be rather common. In fact, many crossings close to the Fermi level in the band structures of ferromagnetic centrosymmetric compounds have been shown to be Weyl nodes.  $\text{Co}_2\text{YZ}$  (with  $\text{Y} = \text{V}, \text{Zr}, \text{Nb}, \text{Ti}, \text{Hf}$ ;  $\text{Z} = \text{Si}, \text{Ge}, \text{Sn}$ )<sup>54,55</sup> and  $\text{Co}_2\text{MnAl}$  (ref. <sup>56</sup>) have all been predicted to be Weyl semimetals with Weyl nodes near the Fermi energy and each having, as a consequence, a giant AHE stemming from the divergent Berry curvature at the Weyl nodes<sup>57</sup>. A large AHE was predicted with Berry curvature calculations<sup>58</sup> and then verified experimentally via transport measurements<sup>59</sup> for the  $\text{Co}_2\text{MnZ}$  ( $\text{Z} = \text{Ga}, \text{Al}$ ) Heusler compounds. Though at the time of the prediction, it was not clear that a large Berry curvature was a consequence of any Weyl nodes or nodal lines, it was speculated that the Dirac crossing in  $\text{Co}_2\text{VSn}$  could be related to a large Berry curvature<sup>58</sup>. Measurements of the AHE in thin films of  $\text{Co}_2\text{MnAl}$  are in good agreement with theory, and in  $\text{Co}_2\text{MnGa}$ , a large anomalous Hall angle up to 12%<sup>59</sup> and a giant anomalous Nernst effect have been observed<sup>60,61</sup>.

Another recently identified Weyl semimetal is the half-metallic magnetic shandite compound  $\text{Co}_3\text{Sn}_2\text{S}_2$  (ref. <sup>62</sup>). Owing to the large Berry curvature in  $\text{Co}_3\text{Sn}_2\text{S}_2$  stemming from its Weyl nodes and weakly gapped nodal lines, as well as due to a relatively low charge conductivity, both the anomalous Hall conductivity and anomalous Hall angle have been measured experimentally to have values of up to  $1,130 \text{ S cm}^{-1}$  and 20%, respectively<sup>62</sup>. This easily grown magnetic Weyl semimetal serves as an ideal platform for studying Weyl physics, and its Berry curvature-induced intrinsic AHE makes it a candidate for finding the QAHE in 2D insulating systems yielding dissipationless edge currents.

Angle-resolved photoemission spectroscopy (ARPES) and scanning tunnelling microscopy experiments revealed intrinsic time-reversal symmetry broken Weyl semimetal states in the Heusler compound  $\text{Co}_2\text{MnGa}$  (ref. <sup>63</sup>) and the shandite compound  $\text{Co}_3\text{Sn}_2\text{S}_2$  (refs. <sup>64,65</sup>). Thus, the connection between the topologically non-trivial states and enhanced Berry curvature of these materials and their observed anomalous transport effects becomes crucial. These materials have natural advantages of high magnetic ordering temperatures, clearly defined topologically non-trivial band structures, low charge carrier densities, and strong electromagnetic responses, and thus show great promise for studying quantum effects, as the design of a material that exhibits a high-temperature QAHE via quantum confinement of a magnetic Weyl semimetal and its integration into quantum devices is the next step. Realization of the QAHE at room temperature would be revolutionary in overcoming limitations of many of today's data-based technologies, which are affected by large electron scattering-induced power losses. Such a discovery would pave the way to a new generation of low-energy consuming quantum electronic and spintronic devices.

In addition to the magnetic Weyl semimetals discussed so far, the Weyl semimetal phase has also been discovered in the non-collinear triangular antiferromagnets  $\text{Mn}_3\text{Z}$  ( $\text{Z} = \text{Ge}, \text{Sn}$ )<sup>66</sup> and  $\text{Mn}_3\text{Ir}$  (ref. <sup>67</sup>).

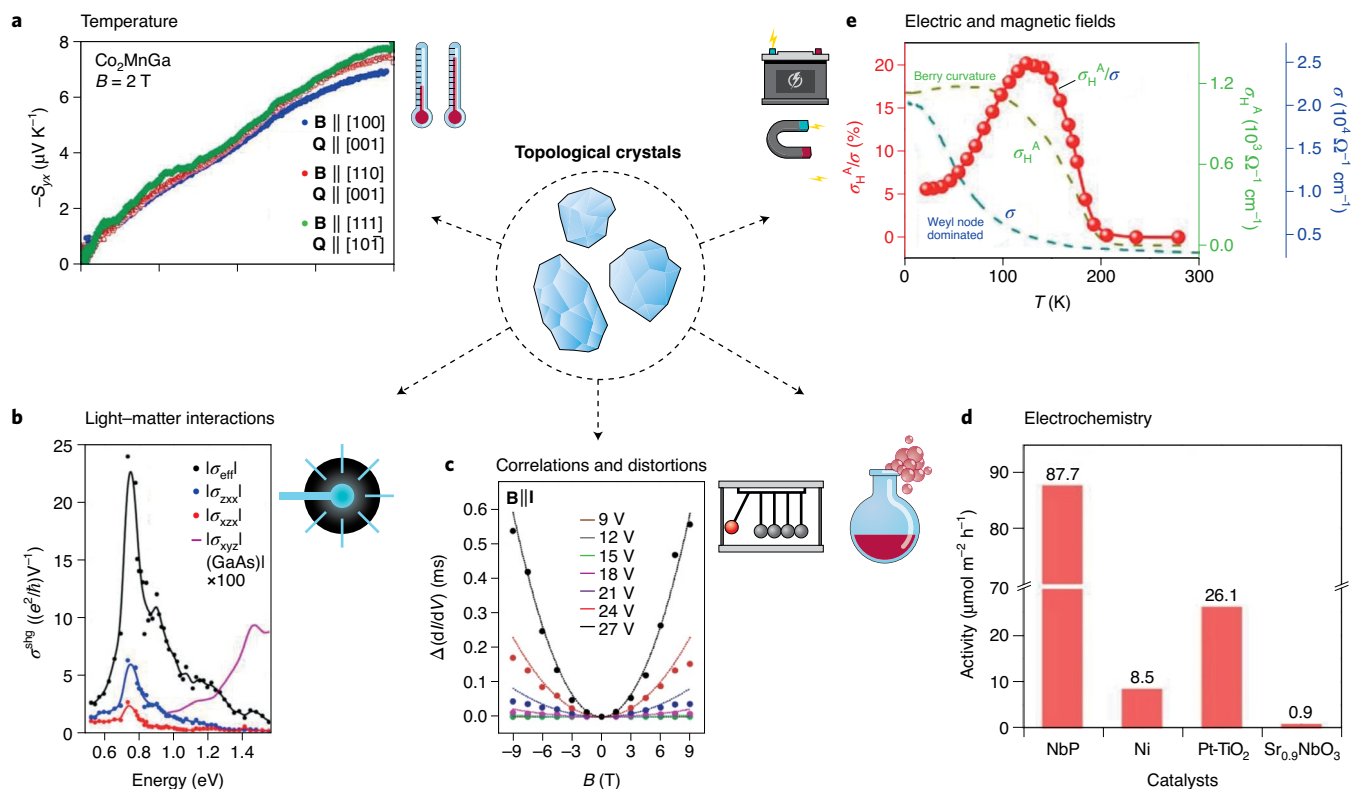


**Fig. 2 | Large responses of topological materials.** Topological materials can exhibit extreme responses to external fields and other stimuli, as illustrated here with experimental results. **a**, Temperature: Nernst signal  $-S_{yx}$  versus temperature in magnetic Weyl semimetal (WSM)  $\text{Co}_2\text{MnGa}$  under a magnetic field  $B = 2$  T. Measurements of the heat current ( $Q$ ) along different crystallographic directions are shown for different applied field directions. The anomalous Nernst effect is the generation of a transverse voltage in a magnetic material due to a thermal gradient and plays a fundamental role in spin-caloritronic devices. **b**, Light-matter interactions: measured second-order nonlinear optical conductivity components  $|\sigma_{\text{zxx}}|$ ,  $|\sigma_{\text{xxz}}|$  and  $|\sigma_{\text{eff}}| = |\sigma_{\text{zxx}} + 4\sigma_{\text{xxz}} + 2\sigma_{\text{xyz}}|$  of non-centrosymmetric WSM TaAs as a function of incident photon energy, with  $|\sigma_{\text{xyz}}|$  of GaAs, is multiplied by 100 and plotted for comparison. **c**, Correlations and distortions: longitudinal magnetoconductance  $\Delta(dI/dV)$  of WSM ( $\text{TaSe}_4$ ) versus magnetic field  $B$  at 80 K for different applied voltages. Well-described by quadratic fits at low magnetic fields, these measurements suggest the presence of an axion phase arising from a charge-density wave gapping the WSM. Theoretical and computational descriptions of such correlations are underway. **d**, Electrochemistry: hydrogen evolution reaction (HER) activities for WSM NbP compared to standard HER catalysts Ni, Pt-TiO<sub>2</sub> and Sr<sub>0.9</sub>NbO<sub>3</sub> scaled by the surface area of the catalysts. The robustness of Fermi arc surface states in WSMs make them a promising material catalyst for electrochemistry, as these states are topologically protected and do not degrade with the surface. **e**, Electric and magnetic fields: anomalous Hall conductivity ( $\sigma_{\text{H}}^A$ ), the charge conductivity ( $\sigma$ ) and the anomalous Hall angle ( $\sigma_{\text{H}}^A/\sigma$ ) of ferromagnetic WSM  $\text{Co}_3\text{Sn}_2\text{S}_2$  at zero magnetic field versus temperature. The anomalous Hall effect describes the formation of a transverse voltage in the absence of a magnetic field when an applied electric field is applied and has been directly linked to the Berry curvature of a material's band structure. Figure reproduced with permission from ref. <sup>60</sup>, Springer Nature Ltd (**a**); ref. <sup>87</sup>, APS (**b**); ref. <sup>88</sup>, Springer Nature Ltd (**c**); ref. <sup>89</sup>, Wiley (**d**); and ref. <sup>62</sup>, Springer Nature Ltd (**e**).

These antiferromagnets similarly have Weyl nodes at the Fermi energy and non-vanishing Berry curvature, and, accordingly, a large AHE has been observed in h-Mn<sub>3</sub>Sn (ref. <sup>68</sup>) and h-Mn<sub>3</sub>Ge (ref. <sup>69</sup>) via magnetotransport investigations even at room temperature. A common understanding is that the AHE is proportional to the magnetization, and in agreement with this simplified picture, the AHE is absent in nearly all antiferromagnets that have zero magnetization. However, the observation of the AHE in these antiferromagnetic Weyl semimetals reveals the deeper connection between the AHE and the Berry curvature, as well as the corresponding correlation between the AHE and Weyl semimetals.

Further, magnetic or magnetically driven Weyl semimetals, which lack time-reversal symmetry, can also offer different avenues of scientific exploration than the inversion-breaking type. Ordinarily, time-reversal symmetry would require a minimum of four Weyl nodes in the material; with this symmetry broken, inversion only requires a single pair, allowing for the possibility of a minimal or ideal Weyl system. A material realization of such electronic structure has been identified in  $\text{EuCd}_2\text{As}_2$ , and it has been suggested

that this minimal Weyl system would be ideal for studying specific contributions to the AHE and other quantum effects.

## Outlook

Looking ahead, we present emerging directions spanning new fermions in chiral crystals, nonlinear optics in Dirac–Weyl semimetals, as well as optically driven and cavity-dressed topological materials science. We anticipate that each of these will grow into a new field in the next few years.

**New fermions in chiral crystals.** Chiral crystals are of special interest because of their unique properties, including their ability to host new fermions (Table 1). In a chiral crystal, the atoms making up the material follow an imaginary spiral staircase-like pattern. While the staircase rotates clockwise in one system, it runs anticlockwise in the counterpart system, and these systems, termed enantiomers, are mirror images of one another. In the P2<sub>1</sub>3 space group (no. 198), of the B20 structure type, the so-called Rarita–Schwinger fermion, which obeys the relativistic field equation for spin-3/2 fermions,

and other multifold fermions resulting from threefold- and sixfold-degenerate band crossings were discovered as new kinds of quasiparticles in candidate materials RhSi, CoSi (ref. <sup>70</sup>) and AlPt (ref. <sup>71</sup>) via ARPES studies.

In conventional Weyl and Dirac semimetals, quasiparticle excitations are described by the Weyl and Dirac equations, respectively, which originate from the different field of high-energy physics. However, in these topologically non-trivial chiral crystals, some of the quasiparticle excitations have no corresponding analogy in high-energy physics and are therefore described as new fermions<sup>72</sup>. Some of these new fermions carry a maximal topological charge or Chern number of 4, which is four times larger than that of the conventional Weyl fermion<sup>71,73</sup>. This leads to several remarkable properties, including a giant quantized circular photogalvanic current, a chiral magnetic effect, and other transport and optical effects which are forbidden in Weyl semimetals. In addition, the electrons on the surfaces of these crystals exhibit a highly unusual helicoid structure that spirals around two high-symmetry momenta, and the complex band topology results in very long Fermi arcs, which are orders of magnitude larger and more robust than those of any known Weyl semimetals. These investigations also find very large topologically non-trivial energy windows, where no trivial bands intersect with the Weyl cones, to be in chiral crystals.

This is an exciting time to be working on topologically non-trivial materials. As shown in Fig. 2, these materials exhibit extreme responses to external stimuli, which is worth exploring further. We now highlight open questions in this field with an emphasis on interdisciplinary topics. Weyl semimetals have shown exceptional promise in just the past few years of active research, and tuning these materials with electrolytic gating using, for example, ionic liquids is of particular interest. This would help elucidate the response of the Weyl nodes under a strong electric field and present yet another avenue to explore the extreme response of these systems. We hypothesize that this response would be quite different from conventional Dirac semimetals. In the spirit of optoelectronic control of topologically non-trivial materials, using these materials in nanophotonic and quantum optical architectures could be rewarding. For example, the low loss in Weyl and Dirac semimetals could make them attractive in nanoplasmonic devices. Similarly, based on the spectral band of response, these materials could be used in spin-photon interfaces coupled with quantum emitters.

In the search for new materials, we observe that the probability of materials with heavy metals and small gaps (<1 eV) being topologically non-trivial is high. Many of these materials also exhibit higher order topologies and new phases like the axion insulator, which has an odd  $Z_2$  classification like normal TIs but is protected not by time-reversal symmetry but by some other symmetry. Questions regarding long-range correlations and the competition between different topologically non-trivial and correlated phases are being tackled via a combination of theory, computation and experiments. We suggest that relativistic effects in materials could also yield magnetic systems beyond the Weyl and Dirac systems discussed here, giving rise to chiral materials that need not be nanostructured to break reciprocity and would have interesting implications for electrochemical applications of topologically non-trivial materials.

**Nonlinear optics with topological materials.** Topologically non-trivial materials also offer a rich material phase space for extending the nonlinear optical effects of graphene, including through the engineering of their topology and Berry connection and curvature<sup>74</sup>. The potential advantages of such materials compared to graphene can be intuitively understood from the band structure. While the extraordinary optoelectronic properties of 2D materials are commonly ‘diluted’ by small overlap with an optical mode, 3D topologically non-trivial materials can have near-unity

overlap with optical modes. Inversion-symmetry breaking Weyl semimetals are of particular interest, as they allow for the generation of even-order nonlinear responses which can be enhanced by divergent Berry curvature at the Weyl nodes. Even-order harmonic generation would be useful, for example, in the applications of photocurrent generation and parametric down conversion used in entangled photon generation. Giant second-harmonic generation<sup>75</sup> and a colossal bulk photovoltaic effect ascribed to a shift current response<sup>76</sup> have already been observed in the inversion symmetry breaking type-I Weyl semimetal TaAs<sup>77</sup> and attributed to Berry curvature effects. Topologically non-trivial materials thus offer substantial improvements over existing nonlinear materials, though the precise combination of topologically non-trivial properties that would produce the strongest nonlinear effects remains an open question.

#### Optically-driven and cavity-dressed topological materials.

Theoretical predictions have revealed pathways towards control of microscopic parameters in complex and topologically non-trivial materials. This includes mode-selective enhancement, control of the amplitude and phase of order parameters, and Floquet-driven symmetry-protected topological edge states. In tandem, numerous experimental advances have investigated electromagnetically induced non-equilibrium states in quantum materials. These include the observation of coherent phonons<sup>78</sup> and Higgs order parameter oscillations<sup>79,80</sup>, vibrationally enhanced transition temperatures in superconductors<sup>81</sup>, the observation of Floquet bands in the TI Bi<sub>2</sub>Se<sub>3</sub>, photoinduced metastability in the charge density wave material 1T-TaS<sub>2</sub> (ref. <sup>82</sup>) and valley selective control in transition metal dichalcogenides<sup>83</sup>. These examples extend to numerous other materials that exhibit a marked sensitivity to small external perturbations<sup>84</sup>. Indeed, the phase space for ‘on-demand’ control of quantum materials is vast both with respect to the materials and modalities that can be pursued<sup>85</sup>. Furthermore, we envision possibilities for dressing topological materials to achieve strong coupling effects, providing yet another pathway to interrogate and manipulate their response<sup>86</sup>.

Light-mediated manipulation of topological quantum matter is particularly attractive, as it enables control at fundamental timescales and access to non-equilibrium states of matter. Ultrafast optical methods have been recently used as a tuning knob to induce insulator-to-metal transitions, topological phases, ferroelectricity, as well as transient superconductivity in copper oxides and organic crystals. This provides a tantalizing opportunity to explore new quantum phases, particularly in the case of transient superconductivity, though key questions remain on the underlying excitation mechanisms, as well as on how to stabilize such short-lived electronic phases. The transient response of topological materials could be measured with advanced optical and scattering methods, such as time-resolved THz spectroscopy and time-resolved resonant inelastic soft X-ray scattering. We expect that a similarly rich set of non-equilibrium phenomena exist in Weyl and Dirac semimetals and axion insulators, making a combination of ideas from topological materials science and driven quantum matter an exciting next step.

Received: 25 January 2020; Accepted: 3 September 2020;

Published online: 2 November 2020

#### References

1. Waldrop, M. M. The 1987 Nobel Prize for Physics: in one of the fastest awards on record, the prize goes to the discoverers of high-temperature superconductivity less than two years after the discovery was made. *Science* **238**, 481–482 (1987).
2. Grünberg, P. A. Nobel Lecture: from spin waves to giant magnetoresistance and beyond. *Rev. Mod. Phys.* **80**, 1531–1540 (2008).
3. Geim, A. K. Nobel Lecture: random walk to graphene. *Rev. Mod. Phys.* **83**, 851–862 (2011).

4. Nakamura, S. Nobel Lecture: background story of the invention of efficient blue InGaN light emitting diodes. *Rev. Mod. Phys.* **87**, 1139–1151 (2015).
5. Haldane, F. D. M. Nobel Lecture: Topological quantum matter. *Rev. Mod. Phys.* **89**, 040502 (2017).
6. Po, H. C., Vishwanath, A. & Watanabe, H. Symmetry-based indicators of band topology in the 230 space groups. *Nat. Commun.* **8**, 50 (2017).
7. Bradlyn, B. et al. Topological quantum chemistry. *Nature* **547**, 298–305 (2017).
8. Watanabe, H., Po, H. C. & Vishwanath, A. Structure and topology of band structures in the 1651 magnetic space groups. *Sci. Adv.* **4**, eaat8685 (2018).
9. Tang, F., Po, H. C., Vishwanath, A. & Wan, X. Efficient topological materials discovery using symmetry indicators. *Nat. Phys.* **15**, 470–476 (2019).
10. Vergniory, M. G. et al. A complete catalogue of high-quality topological materials. *Nature* **566**, 480–485 (2019).
11. Tang, F., Po, H. C., Vishwanath, A. & Wan, X. Comprehensive search for topological materials using symmetry indicators. *Nature* **566**, 486–489 (2019).
12. Zhou, X. et al. Topological crystalline insulator states in the  $\text{Ca}_2\text{As}$  family. *Phys. Rev. B* **98**, 241104 (2018).
13. Kane, C. L. & Mele, E. J.  $Z_2$  topological order and the quantum spin Hall effect. *Phys. Rev. Lett.* **95**, 146802 (2005).
14. Hasan, M. Z. & Kane, C. L. Colloquium: topological insulators. *Rev. Mod. Phys.* **82**, 3045–3067 (2010).
15. Qi, X.-L. & Zhang, S.-C. Topological insulators and superconductors. *Rev. Mod. Phys.* **83**, 1057–1110 (2011).
16. Maciejko, J., Hughes, T. L. & Zhang, S.-C. The quantum spin Hall effect. *Annu. Rev. Condens. Matter Phys.* **2**, 31–53 (2011).
17. Hasan, M. Z. & Moore, J. E. Three-dimensional topological insulators. *Annu. Rev. Condens. Matter Phys.* **2**, 55–78 (2011).
18. Fu, L. & Kane, C. L. Topological insulators with inversion symmetry. *Phys. Rev. B* **76**, 045302 (2007).
19. Kane, C. L. & Mele, E. J. Quantum spin Hall effect in graphene. *Phys. Rev. Lett.* **95**, 226801 (2005).
20. Bernevig, B. A., Hughes, T. L. & Zhang, S.-C. Quantum spin Hall effect and topological phase transition in HgTe quantum wells. *Science* **314**, 1757–1761 (2006).
21. König, M. et al. Quantum spin Hall insulator state in HgTe quantum wells. *Science* **318**, 766–770 (2007).
22. Zhang, H. et al. Topological insulators in  $\text{Bi}_2\text{Se}_3$ ,  $\text{Bi}_2\text{Te}_3$  and  $\text{Sb}_2\text{Te}_3$  with a single Dirac cone on the surface. *Nat. Phys.* **5**, 438–442 (2009).
23. Xia, Y. et al. Observation of a large-gap topological-insulator class with a single Dirac cone on the surface. *Nat. Phys.* **5**, 398–402 (2009).
24. Chadov, S. et al. Tunable multifunctional topological insulators in ternary Heusler compounds. *Nat. Mater.* **9**, 541–545 (2010).
25. Lin, H. et al. Half-Heusler ternary compounds as new multifunctional experimental platforms for topological quantum phenomena. *Nat. Mater.* **9**, 546–549 (2010).
26. Shekhar, C. et al. Ultrahigh mobility and nonsaturating magnetoresistance in Heusler topological insulators. *Phys. Rev. B* **86**, 155314 (2012).
27. Rasche, B. et al. Stacked topological insulator built from bismuth-based graphene sheet analogues. *Nat. Mater.* **12**, 422–425 (2013).
28. Liang, A. J. et al. Observation of the topological surface state in the nonsymmorphic topological insulator  $\text{KHgSb}$ . *Phys. Rev. B* **96**, 165143 (2017).
29. Ma, J. et al. Experimental evidence of hourglass fermion in the candidate nonsymmorphic topological insulator  $\text{KHgSb}$ . *Sci. Adv.* **3**, e1602415 (2017).
30. Zhang, X., Zhang, H., Wang, J., Felser, C. & Zhang, S.-C. Actinide topological insulator materials with strong interaction. *Science* **335**, 1464–1466 (2012).
31. Yan, B., Muehler, L., Qi, X.-L., Zhang, S.-C. & Felser, C. Topological insulators in filled skutterudites. *Phys. Rev. B* **85**, 165125 (2012).
32. Yan, B., Jansen, M. & Felser, C. A large-energy-gap oxide topological insulator based on the superconductor  $\text{BaBiO}_3$ . *Nat. Phys.* **9**, 709–711 (2013).
33. Tokura, Y., Yasuda, K. & Tsukazaki, A. Magnetic topological insulators. *Nat. Rev. Phys.* **1**, 126–143 (2019).
34. Wan, X., Turner, A. M., Vishwanath, A. & Savrasov, S. Y. Topological semimetal and Fermi-arc surface states in the electronic structure of pyrochlore iridates. *Phys. Rev. B* **83**, 205101 (2011).
35. Burkov, A. A., Hook, M. D. & Balents, L. Topological nodal semimetals. *Phys. Rev. B* **84**, 235126 (2011).
36. Young, S. M. et al. Dirac semimetal in three dimensions. *Phys. Rev. Lett.* **108**, 140405 (2012).
37. Wang, Z. et al. Dirac semimetal and topological phase transitions in  $\text{A}_3\text{Bi}$  ( $\text{A} = \text{Na}, \text{K}, \text{Rb}$ ). *Phys. Rev. B* **85**, 195320 (2012).
38. Weng, H., Fang, C., Fang, Z., Bernevig, B. A. & Dai, X. Weyl semimetal phase in noncentrosymmetric transition-metal monophosphides. *Phys. Rev. X* **5**, 011029 (2015).
39. Xu, S.-Y. et al. Discovery of a Weyl fermion semimetal and topological Fermi arcs. *Science* **349**, 613–617 (2015).
40. Lv, B. Q. et al. Experimental discovery of Weyl semimetal TaAs. *Phys. Rev. X* **5**, 031013 (2015).
41. Yang, L. X. et al. Weyl semimetal phase in the non-centrosymmetric compound TaAs. *Nat. Phys.* **11**, 728–732 (2015).
42. Jiang, J. et al. Signature of type-II Weyl semimetal phase in MoTe. *Nat. Commun.* **8**, 13973 (2017).
43. Liu, Z. K. et al. Discovery of a three-dimensional topological Dirac semimetal,  $\text{Na}_3\text{Bi}$ . *Science* **343**, 864–867 (2014).
44. Wang, Z., Weng, H., Wu, Q., Dai, X. & Fang, Z. Three-dimensional Dirac semimetal and quantum transport in  $\text{Cd}_3\text{As}_2$ . *Phys. Rev. B* **88**, 125427 (2013).
45. Armitage, N. P., Mele, E. J. & Vishwanath, A. Weyl and Dirac semimetals in three-dimensional solids. *Rev. Mod. Phys.* **90**, 015001 (2018).
46. Nielsen, H. B. & Ninomiya, M. The Adler-Bell-Jackiw anomaly and Weyl fermions in a crystal. *Phys. Lett. B* **130**, 389–396 (1983).
47. Zyuzin, A. A. & Burkov, A. A. Topological response in Weyl semimetals and the chiral anomaly. *Phys. Rev. B* **86**, 115133 (2012).
48. Xu, G., Weng, H., Wang, Z., Dai, X. & Fang, Z. Chern semimetal and the quantized anomalous Hall effect in  $\text{HgCr}_2\text{Se}_4$ . *Phys. Rev. Lett.* **107**, 186806 (2011).
49. Ueda, K. et al. Magnetic-field induced multiple topological phases in pyrochlore iridates with Mott criticality. *Nat. Commun.* **8**, 15515 (2017).
50. Ueda, K. et al. Spontaneous Hall effect in the Weyl semimetal candidate of all-in-all-out pyrochlore iridate. *Nat. Commun.* **9**, 3032 (2018).
51. LaBarre, P. G., Dong, L., Trinh, J., Siegrist, T. & Ramirez, A. P. Evidence for undoped Weyl semimetal charge transport in  $\text{Y}_2\text{Ir}_2\text{O}_7$ . *J. Phys. Condens. Matter* **32**, 02LT01 (2019).
52. Hirschberger, M. et al. The chiral anomaly and thermopower of Weyl fermions in the half-Heusler  $\text{GdPtBi}$ . *Nat. Mater.* **15**, 1161–1165 (2016).
53. Shekhar, C. et al. Anomalous Hall effect in Weyl semimetal half-Heusler compounds  $\text{RPtBi}$  ( $\text{R} = \text{Gd}$  and  $\text{Nd}$ ). *Proc. Natl Acad. Sci. USA* **115**, 9140–9144 (2018).
54. Wang, Z. et al. Time-reversal-breaking Weyl fermions in magnetic heusler alloys. *Phys. Rev. Lett.* **117**, 236401 (2016).
55. Chang, G. et al. Room-temperature magnetic topological Weyl fermion and nodal line semimetal states in half-metallic Heusler  $\text{CoTiX}$  ( $\text{X} = \text{Si}, \text{Ge}, \text{or Sn}$ ). *Sci. Rep.* **6**, 38839 (2016).
56. Kübler, J. & Felser, C. Weyl points in the ferromagnetic Heusler compound  $\text{Co}_2\text{MnAl}$ . *Europhys. Lett.* **114**, 47005 (2016).
57. Burkov, A. A. Anomalous Hall effect in Weyl metals. *Phys. Rev. Lett.* **113**, 187202 (2014).
58. Kübler, J. & Felser, C. Berry curvature and the anomalous Hall effect in Heusler compounds. *Phys. Rev. B* **85**, 012405 (2012).
59. Manna, K. et al. From colossal to zero: controlling the anomalous Hall effect in magnetic Heusler compounds via Berry curvature design. *Phys. Rev. X* **8**, 041045 (2018).
60. Sakai, A. et al. Giant anomalous Nernst effect and quantum-critical scaling in a ferromagnetic semimetal. *Nat. Phys.* **14**, 1119–1124 (2018).
61. Guin, S. N. et al. Anomalous Nernst effect beyond the magnetization scaling relation in the ferromagnetic Heusler compound  $\text{Co}_2\text{MnGa}$ . *npj Asia Mater.* **11**, 16 (2019).
62. Liu, E. et al. Giant anomalous Hall effect in a ferromagnetic kagome-lattice semimetal. *Nat. Phys.* **14**, 1125–1131 (2018).
63. Belopolski, I. et al. Discovery of topological Weyl fermion lines and drumhead surface states in a room temperature magnet. *Science* **365**, 1278–1281 (2019).
64. Liu, D. F. et al. Magnetic Weyl semimetal phase in a kagomé crystal. *Science* **365**, 1282–1285 (2019).
65. Morali, N. et al. Fermi-arc diversity on surface terminations of the magnetic Weyl semimetal  $\text{Co}_3\text{Sn}_2\text{S}_2$ . *Science* **365**, 1286–1291 (2019).
66. Kübler, J. & Felser, C. Non-collinear antiferromagnets and the anomalous Hall effect. *Europhys. Lett.* **108**, 67001 (2014).
67. Chen, H., Niu, Q. & MacDonald, A. H. Anomalous Hall effect arising from noncollinear antiferromagnetism. *Phys. Rev. Lett.* **112**, 017205 (2014).
68. Nakatsuji, S., Kiyohara, N. & Higo, T. Large anomalous Hall effect in a non-collinear antiferromagnet at room temperature. *Nature* **527**, 212–215 (2015).
69. Nayak, A. K. et al. Large anomalous Hall effect driven by a nonvanishing Berry curvature in the noncollinear antiferromagnet  $\text{Mn}_3\text{Ge}$ . *Sci. Adv.* **2**, e1501870 (2016).
70. Sanchez, D. S. et al. Topological chiral crystals with helicoid-arc quantum states. *Nature* **567**, 500–505 (2019).
71. Schröter, N. B. M. et al. Chiral topological semimetal with multifold band crossings and long Fermi arcs. *Nat. Phys.* **15**, 759–765 (2019).
72. Bradlyn, B. et al. Beyond Dirac and Weyl fermions: Unconventional quasiparticles in conventional crystals. *Science* **353**, aaf5037 (2016).
73. Schröter, N. B. M. et al. Observation and control of maximal Chern numbers in a chiral topological semimetal. *Science* **369**, 179–183 (2020).
74. Cook, A. M., Fregoso, B. M., de Juan, F., Coh, S. & Moore, J. E. Design principles for shift current photovoltaics. *Nat. Commun.* **8**, 14176 (2017).
75. Wu, L. et al. Giant anisotropic nonlinear optical response in transition metal monpnictide Weyl semimetals. *Nat. Phys.* **13**, 350–355 (2016).
76. Osterhoudt, G. B. et al. Colossal mid-infrared bulk photovoltaic effect in a type-I Weyl semimetal. *Nat. Mater.* **18**, 471–475 (2019).

77. Garcia, C. A. C., Coulter, J. & Narang, P. Optoelectronic response of the type-I Weyl semimetals TaAs and NbAs from first principles. *Phys. Rev. Res.* **2**, 013073 (2020).
78. Lindenberg, A. M. et al. Time-resolved X-Ray diffraction from coherent phonons during a laser-induced phase transition. *Phys. Rev. Lett.* **84**, 111–114 (2000).
79. Matsunaga, R. et al. Light-induced collective pseudospin precession resonating with Higgs mode in a superconductor. *Science* **345**, 1145–1149 (2014).
80. Juraschek, D. M., Meier, Q. N. & Narang, P. Parametric excitation of an optically silent goldstone-like phonon mode. *Phys. Rev. Lett.* **124**, 117401 (2020).
81. Mitran, M. et al. Possible light-induced superconductivity in  $K_3C_{60}$  at high temperature. *Nature* **530**, 461–464 (2016).
82. Scruby, C. B., Williams, P. M. & Parry, G. S. The role of charge density waves in structural transformations of 1T TaS<sub>2</sub>. *Philos. Mag.* **31**, 255–274 (1975).
83. Shin, D. et al. Phonon-driven spin-Floquet magneto-valleytronics in MoS<sub>2</sub>. *Nat. Commun.* **9**, 638 (2018).
84. He, R.-H. et al. From a single-band metal to a high-temperature superconductor via two thermal phase transitions. *Science* **331**, 1579–1583 (2011).
85. Basov, D. N., Averitt, R. D. & Hsieh, D. Towards properties on demand in quantum materials. *Nat. Mater.* **16**, 1077–1088 (2017).
86. Rivera, N., Flick, J. & Narang, P. Variational theory of nonrelativistic quantum electrodynamics. *Phys. Rev. Lett.* **122**, 193603 (2019).
87. Patankar, S. et al. Resonance-enhanced optical nonlinearity in the Weyl semimetal TaAs. *Phys. Rev. B* **98**, 359 (2018).
88. Gooth, J. et al. Axionic charge-density wave in the Weyl semimetal (TaSe)<sub>2</sub>. *Nature* **575**, 315–319 (2019).
89. Rajamathi, C. R. et al. Weyl semimetals as hydrogen evolution catalysts. *Adv. Mater.* **29**, (2017).
90. Yan, B. & Felser, C. Topological materials: Weyl semimetals. *Annu. Rev. Condens. Matter Phys.* **8**, 337–354 (2017).

### Acknowledgements

We thank M. Hopkins (Harvard University), D. Nenno (Harvard University), Y. Wang (Harvard University) and J. Gooth (Max Planck) for fruitful discussions and feedback. P.N. acknowledges helpful discussions with D. Basov (Columbia University) and S. Parkin (Max Planck) on various aspects of this work. This work was supported by the DOE Photonics at Thermodynamic Limits Energy Frontier Research Center under grant no. DE-SC0019140. C.A.C.G. is supported by the NSF Graduate Research Fellowship Program under grant no. DGE-1745303. P.N. is a Moore Inventor Fellow and gratefully acknowledges support through grant GBMF8048 from the Gordon and Betty Moore Foundation, and support as a CIFAR Azrieli Global Scholar.

### Author contributions

P.N., C.A.C.G. and C.F. have all contributed equally to this Perspective, the writing and the ideas presented here.

### Competing interests

The authors declare no competing interests.

### Additional information

Correspondence should be addressed to P.N.

Reprints and permissions information is available at [www.nature.com/reprints](http://www.nature.com/reprints).

**Publisher's note** Springer Nature remains neutral with regard to jurisdictional claims in published maps and institutional affiliations.

© Springer Nature Limited 2020